

Measurement of the $p(\gamma, \pi^0)$ Cross Section at Threshold

R. Beck,^(a) F. Kalleicher, B. Schoch,^(b) and J. Vogt^(c)

Institut für Kernphysik, Universität Mainz, D-6500 Mainz, West Germany

G. Koch,^(d) H. Ströher, and V. Metag

II. Physikalisches Institut, Universität Giessen, D-6300 Giessen, West Germany

J. C. McGeorge, J. D. Kellie, and S. J. Hall

Kelvin Laboratory, University of Glasgow, United Kingdom

(Received 4 May 1990; revised manuscript received 23 July 1990)

Differential and absolute cross sections for the reaction $p(\gamma, \pi^0)$ have been measured with energy-defined photons in the threshold region ($E_\gamma = 131.4\text{--}157.2$ MeV). The E_{0+} amplitude has been extracted out of the data. The values found are in disagreement with predictions of low-energy theorems.

PACS numbers: 13.60.Le, 25.20.Lj

Low-energy theorems (LETs) based on gauge invariance and the partial conservation of the axial-vector current have been used to make model-independent predictions for the photoproduction of pions from nucleons. Good agreement with the experimental data on charged-pion photoproduction was taken as evidence for the validity of the underlying fundamental assumptions.

However, drastic deviations from the LET predictions have been found in a recent measurement of neutral-pion photoproduction performed with the Saclay Linac.¹ The discrepancy with the theoretical predictions becomes even more pronounced with the present experiment measuring angular distributions of neutral pions, to which the theoretical predictions are very sensitive.

The differential photoproduction cross section close to threshold is dominated by s and p waves. The s -wave photoproduction amplitude E_{0+} (this abbreviation will be used throughout the text for $E_{0+}^{p\pi^0}$) is uniquely given by LET up to $\mu^2 = (m_\pi/M_N)^2$ (m_π denotes the pion mass; M_N denotes the nuclear mass). In an attempt to reconcile the LET prediction with the experimental result of Ref. 1, the influence of corrections due to rescattering effects,²⁻⁵ virtual excitations of nucleon resonances, and meson exchange in the t channel has been investigated, in addition to contributions due to chiral-symmetry breaking on the quark level.⁶ In consequence, previous calculations of rescattering contributions⁷ used in order to extract the LET-constrained E_{0+} amplitude have been challenged.

In this Letter we present data on the differential and total cross sections from threshold to 10 MeV above threshold at five different energies. The experiment was performed at the Mainz Microtron MAMI A,⁸ using a tagging facility⁹ in combination with a π^0 spectrometer.¹⁰ A cw electron beam of 183.5 MeV, provided by MAMI A, was used to produce photons with well defined energies (FWHM=0.28 MeV) by means of bremsstrahlung tagging. In the energy range 131.4–157.2 MeV the

tagged-photon flux was $1 \times 10^7/\text{s}$. The π^0 spectrometer consisted of two arrays of lead-glass detectors placed horizontally on either side of the beam at a distance of 50 cm from a liquid-hydrogen target. The arrays contained a total of 88 separate lead-glass detectors. The angle between the centroid of the blocks and the γ beam was chosen to be 80° . In this configuration the complete π^0 angular distribution $0 \leq \theta \leq 180^\circ$ was covered for the given tagging range. The absolute detection efficiency and the angular acceptances have been determined using Monte Carlo simulations which were checked by measurements of the $^{12}\text{C}(\gamma, \pi^0)^{12}\text{C}$ reaction. The p -wave nature of this coherent process, within 4.4 MeV above the production threshold, provided a characteristic angular distribution. The absolute energy calibration of the tagging spectrometer was checked by measuring the known energy of the MAMI beam directly using the spectrometer and by the determination of the threshold of the process $^{12}\text{C}(\gamma, \pi^0)^{12}\text{C}$. From these separate measurements the uncertainty in the energy of the tagged photons was estimated to be 220 keV. The target thickness of 11 cm together with the tagged-photon flux of $1 \times 10^7/\text{s}$ provided a luminosity of $4.6 \times 10^{30} \text{ s}^{-1} \text{ cm}^{-2}$.

Neutral pions were identified event by event by a cut in a two-dimensional plot of the tagged energy versus opening angle of the decay photons. Random events were subtracted using appropriate cuts in the time spectra. Figure 1 shows the total cross section as a function of the photon energy together with the data obtained by Mazzucato *et al.*¹ There is agreement within the experimental error bars. The differential cross sections for five energy intervals around photon energies $E_\gamma = 146.8, 149.1, 151.4, 153.7,$ and 156.1 MeV are shown in Figs. 2(a)–2(e).

The absolute overall systematic error amounts to 7.5%, due to the uncertainty in the luminosity, the π^0 detection efficiency, and dead-time corrections. The experiment was performed at one setting of the spectrome-

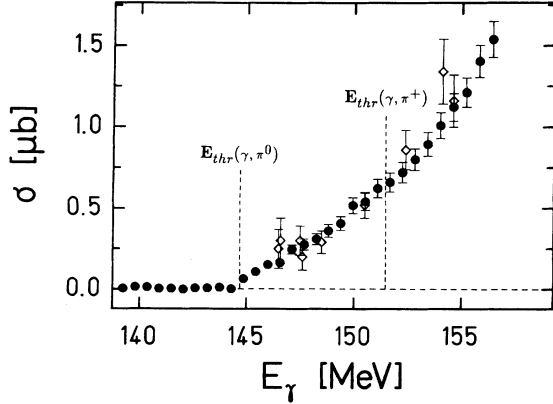


FIG. 1. Total cross section for the reaction $p(\gamma, \pi_0)$. Solid circles, this work; open rhombi, Ref. 1.

ter and incoming electron energy. Consequently, relative uncertainties in the energy dependence as well as the angular distribution were minimized. Using this data base, which is a factor of 10 larger than the previous measurement, the extraction of the E_{0+} amplitude as a function of energy has been accomplished in essentially a model-independent way. Since close to threshold only $l=0,1$ partial waves are important, the differential cross section can be parametrized according to

$$\frac{d\sigma}{d\Omega} = \frac{q}{k} (A + B \cos\theta + C \cos^2\theta). \quad (1)$$

Here q and k are the momentum of the pion and the photon, respectively, and θ is the emission angle of the π^0 in the c.m. system relative to the photon momentum. A , B , and C are functions of the complex multipoles E_{0+} , M_{1+} , M_{1-} , and E_{1+} . The angular distribution coefficients have been determined by fits to the angular distributions and are listed in Table I.

The s -wave amplitude E_{0+} and the p -wave amplitude $M_1 = 3E_{1+} + M_{1+} - M_{1-}$ can be determined from the following symmetrical system of equations:

$$A + C = E_{0+}^2 - M_1^2, \quad (2)$$

$$B = 2 \operatorname{Re}(E_{0+} M_1). \quad (3)$$

Assuming the imaginary part of the amplitudes can be neglected compared to the real one (e.g., a contribution of the imaginary part as large as calculated in Ref. 2 would change the result by 3.5% in the worst case), the solutions are

$$E_{0+}, M_1 = \frac{1}{2} (\pm \sqrt{A+B+C} \pm \sqrt{A-B+C}), \quad (4)$$

which can be labeled $E_{0+}^{(++)}$, $E_{0+}^{(+-)}$, $E_{0+}^{(-+)}$, and $E_{0+}^{(--)}$ in an obvious notation (analogously for M_1). Since the experimental B coefficient is negative for all incident photon energies (see Table I) $A+B+C$ is always smaller than $A-B+C$. In addition E_{0+} and M_1 have different signs because of Eq. (3). Only the following com-

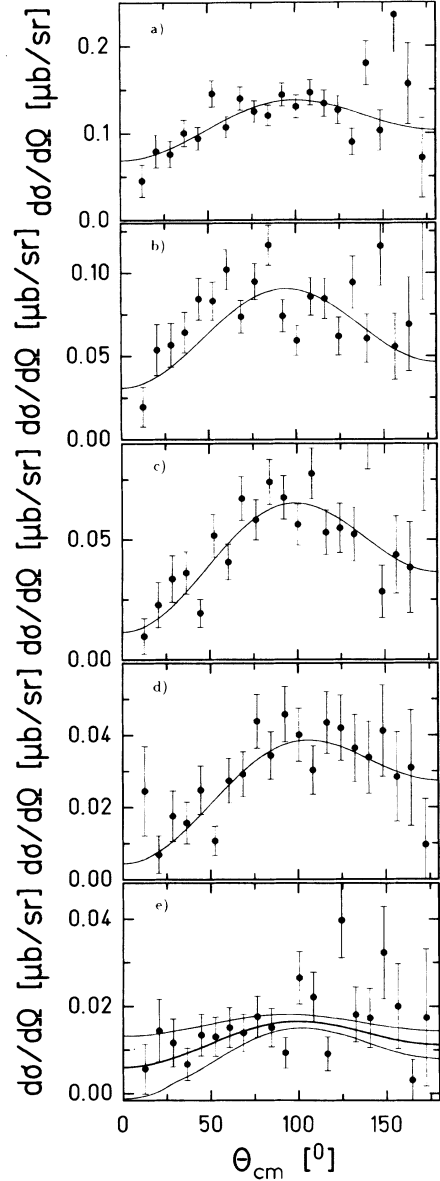


FIG. 2. Differential cross sections. The curves are the result of a fit to the data (for $E_\gamma = 146.8$ MeV, the $\pm 1\sigma$ results are also plotted). (a) $E_\gamma = 156.1$ MeV, (b) $E_\gamma = 153.7$ MeV, (c) $E_\gamma = 151.4$ MeV, (d) $E_\gamma = 149.1$ MeV, (e) $E_\gamma = 146.8$ MeV.

binations are allowed: (i) For $E_{0+} > 0$, $M_1 < 0$,

$$(E_{0+}^{(++)}, M_1^{(+-)}), \text{ if } |E_{0+}| > |M_1|, \quad (5a)$$

$$(E_{0+}^{(-+)}, M_1^{(--)}) , \text{ if } |E_{0+}| < |M_1|;$$

(ii) for $E_{0+} < 0$, $M_1 > 0$,

$$(E_{0+}^{(--)}, M_1^{(-+)}) , \text{ if } |E_{0+}| > |M_1|, \quad (5b)$$

$$(E_{0+}^{(+-)}, M_1^{(++)}) , \text{ if } |E_{0+}| < |M_1|.$$

Since $E_{0+}^{(xx)} = M_1^{(xx)}$ ($x = +, -$), two combinations of

TABLE I. Results of the fit for the coefficients A , B , and C defined in Eq. (1).

E_γ (MeV)	A ($\mu\text{b}/\text{sr}$)	B ($\mu\text{b}/\text{sr}$)	C ($\mu\text{b}/\text{sr}$)
146.8	0.099 ± 0.011	-0.0158 ± 0.012	-0.047 ± 0.021
149.1	0.158 ± 0.011	-0.049 ± 0.012	-0.09 ± 0.022
151.4	0.225 ± 0.012	-0.044 ± 0.013	-0.141 ± 0.025
153.7	0.277 ± 0.012	-0.024 ± 0.016	-0.158 ± 0.027
156.1	0.376 ± 0.014	-0.048 ± 0.018	-0.139 ± 0.033

solutions are finally obtained, which are mirror symmetric. If one chooses (i) or (ii), a *unique* solution is found, provided it is known whether $|E_{0+}|$ is greater or less than $|M_1|$. The amplitudes obtained according to this prescription are plotted as solid circles (squares) in Fig. 3 as a function of qk (the mirror-symmetric solution has been omitted for clarity). Obviously the positive and linearly increasing solution should be identified with the p -wave amplitudes (a p wave close to threshold being proportional to qk , i.e., solution $M_1^{(++)}$) because of the dominant M_{1+} amplitude, while the negative and almost constant data set is the s -wave amplitude (i.e., solution $E_{0+}^{(-)}$). Here, it has been assumed that $|M_1| > |E_{0+}|$ for *all* energies (solid symbols in Fig. 3); in the following this data set is named solution I. Because of the different energy dependences of s - and p -wave amplitudes, $|M_1|$ will become smaller than $|E_{0+}|$ at some qk close to threshold. In this case the combination ($E_{0+}^{(-)}, M_1^{(-)}$) has to be used (see above). This change of signs ensures the correct threshold behavior of E_{0+} , i.e., $E_{0+}^2 = A$ and $B = C = 0$.

However, there are strong indications in our data [based, for example, on the ratio $B/(A+C)$] that the switching among solutions occurs between our data points at $E_\gamma = 149.1$ and 151.4 MeV, i.e., near the π^+ production threshold of 151.4 MeV, although our results are not precise enough to definitely exclude the solution with no change in the covered energy range. We have, therefore, included a second data set for E_{0+} in Fig. 3 (open circles, open squares) and Table II (solution II). Solutions I and II coincide for energies above the charged-pion threshold. Below this threshold the solution $E_{0+}^{(-)}$ yields values for the s -wave amplitude which are strongly enhanced and could be due to rescattering through a charged intermediate pion. However, with this solution the simple qk dependence of the M_1 amplitude is destroyed below the (γ, π^+) threshold. In any case a dramatic discrepancy between the LET prediction ($E_{0+} = -2.5 \times 10^{-3}/m_\pi$) and our experimental result (see Table II) is clearly established *at* and above the π^+ threshold energy where effects due to rescattering are minimized in the real part of the E_{0+} amplitude.

The prediction of Nozawa *et al.*² which includes rescattering effects in a dynamical model is plotted in Fig. 3. It turns out that this calculation is not able to repro-

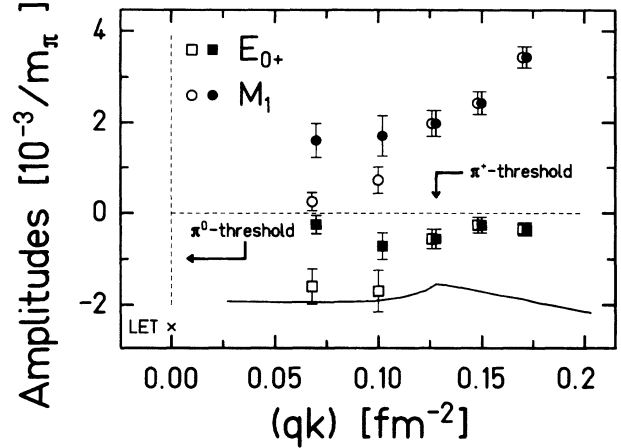


FIG. 3. Results for E_{0+} (see Table II) and the corresponding M_1 plotted as a function of qk . Solid squares (circles), solution I; open squares (circles), solution II (see text). At $qk=0$ the LET prediction is indicated. The solid line is the prediction of Ref. 2.

duce the experimental data for energies above the (γ, π^+) threshold. Calculations which include, in a self-consistent manner, rescattering effects as well as chiral-symmetry breaking on the current-quark-mass level would perhaps be able to describe the data.¹¹

The sum of the p -wave multipoles, entering in Eqs. (2)–(5), yields, for solution I, an average value of $\langle M_1 \rangle = (8.3 \pm 0.2) \times 10^{-3} qk/m_\pi^3$ in agreement with the result reported in Ref. 1. A detailed evaluation of these multipoles will be published in a forthcoming paper.

Summarizing, the E_{0+} amplitude for neutral-pion production from the proton has been determined for several energies near the production threshold, and previously reported deviations from LET are confirmed by good-statistics angular distribution data. However, a certain ambiguity remains for our two low-energy points (solutions I and II). In model calculations the p wave should be calculated in order to compare with the measured cross sections.

Furthermore, the present Letter demonstrates that

TABLE II. The extracted values for E_{0+} by using Eqs. (2)–(5) and the fit coefficients of Table I. First column: solution I, assuming that $E_{0+} < 0$, $M_1 > 0$, and $|M_1| > |E_{0+}|$ for *all* energies ($E_{0+}^{(-)}$, see text). Second column: solution II, assuming that $|M_1| > |E_{0+}|$ for $E_\gamma > 151.4$ MeV ($E_{0+}^{(-)}$) while $|M_1| < |E_{0+}|$ for $E_\gamma < 151.4$ MeV ($E_{0+}^{(-)}$).

E_γ (MeV)	E_{0+}^+ ($10^{-3}/m_\pi$)	E_{0+}^- ($10^{-3}/m_\pi$)
146.8	-0.25 ± 0.19	-1.61 ± 0.16
149.1	-0.72 ± 0.17	-1.69 ± 0.18
151.4	-0.56 ± 0.13	-0.56 ± 0.13
153.7	-0.26 ± 0.17	-0.26 ± 0.17
156.1	-0.35 ± 0.13	-0.35 ± 0.13

with the new cw facilities which are currently working or proposed for the future, new classes of experiments can be performed. Of great importance will be a measurement of the reaction $n(\gamma, \pi^0)$ which, together with measurements of charged-pion production, will allow isospin violation in the threshold region to be investigated for the first time. In particular, since the isoscalar and isospin even multipoles show a special sensitivity to the chiral-breaking terms in the interaction,¹² studies of these specific parts of the interaction will become feasible.

We would like to thank K. H. Kaiser and the operator staff of the MAMI A accelerator for providing the excellent and stable electron beams. We acknowledge many fruitful discussions with D. Drechsel, J. Friedrich, and L. Tiator. This work was supported in part by Deutsche Forschungsgemeinschaft Sonderforschungsbereich No. 201.

^(a)Present address: Massachusetts Institute of Technology,

Cambridge, MA 02139.

^(b)Now at University of Bonn, Bonn, Germany.

^(c)Now at University of Saskatchewan, Saskatoon, Canada S7N 0W0.

^(d)Now at DuPont Co., West Germany.

¹E. Mazzucato *et al.*, Phys. Rev. Lett. **57**, 3144 (1986).

²S. Nozawa *et al.*, Phys. Rev. C **41**, 213 (1990).

³S. N. Yang, Phys. Rev. C **40**, 1810 (1989).

⁴M. Araki, Phys. Lett. B **219**, 135 (1989).

⁵A. N. Kamal, Phys. Rev. Lett. **63**, 2364 (1989).

⁶L. M. Nath and S. K. Singh, Phys. Rev. C **39**, 1207 (1989).

⁷J. M. Laget, Phys. Rep. **69**, 1 (1981).

⁸H. Herminghaus *et al.*, Nucl. Instrum. Methods **138**, 1 (1976).

⁹J. D. Kellie *et al.*, Nucl. Instrum. Methods Phys. Res., Sect. A **241**, 153 (1985).

¹⁰H. Ströher *et al.*, Nucl. Instrum. Methods Phys. Res., Sect. A **269**, 568 (1988).

¹¹D. Drechsel and M. M. Giannini, Rep. Prog. Phys. **52**, 1083 (1989).

¹²G. Furlan *et al.*, Nuovo Cimento **20**, 118 (1974).